Total reflection high-energy positron diffraction: An ideal diffraction technique for surface structure analysis

2014 Appl. Phys. Express 7 056601

(http://iopscience.iop.org/1882-0786/7/5/056601)

Applied Physics Express 7, 056601 (2014)
http://dx.doi.org/10.7567/APEX.7.056601

Total reflection high-energy positron diffraction: An ideal diffraction technique for surface structure analysis

Yuki Fukaya[1], Masaki Maekawa[1], Atsuo Kawasuso[1], Izumi Mochizuki[2], Ken Wada[2], Tetsuo Shidara[3], Ayahiko Ichimiya[4], and Toshio Hyodo[2]*

[1]*Advanced Science Research Center, Japan Atomic Energy Agency, Takasaki, Gunma 370-1292, Japan*
[2]*Institute of Materials Structure Science, High Energy Accelerator Research Organization (KEK), Tsukuba, Ibaraki 305-0801, Japan*
[3]*Accelerator Laboratory, High Energy Accelerator Research Organization (KEK), Tsukuba, Ibaraki 305-0801, Japan*
[4]*Nagoya University, Nagoya 464-8601, Japan*
E-mail: toshio.hyodo@kek.jp

Received February 12, 2014; accepted March 19, 2014; published online April 9, 2014

It is shown that the reflection high-energy positron diffraction (RHEPD) pattern from a Si(111)-(7 × 7) reconstructed surface for the total reflection condition, that is, the total reflection high-energy positron diffraction (TRHEPD) pattern, does not contain contributions from atoms in the bulk. Now, a method of observing the diffraction pattern formed only by the atoms on the topmost surface by a straightforward measurement of a bulk sample is available.

Definitive knowledge of the crystal structure of materials is key to our understanding of their physical and chemical properties and their technological applications. X-ray diffraction has long been the standard technique in materials research to elucidate the bulk structure. However, for the determination of the top and near-surface atomic configurations, an equivalent single method is yet to be established. Here, we show that total reflection high-energy positron diffraction (TRHEPD) is an ideal technique for this purpose, where full use is made of the total reflection of the positron beam from a solid surface in reflection high-energy positron diffraction (RHEPD),[1,2] the positron counterpart of reflection high-energy electron diffraction (RHEED).[3]

The positron, the antiparticle of the electron, has the same properties as the electron except that it is positive in charge. Its eventual annihilation with an electron into γ-rays has been employed in various applications based on the detection of these annihilation γ-rays. Examples include positron emission tomography (PET) for locating cancers in the human body, angular correlation of annihilation radiation (ACAR) for the investigation of Fermi surfaces of metals and alloys, and positron lifetime measurements for finding vacancy-type defects in materials.

The way positrons are used in diffraction techniques differs from that in the applications listed above in that, here, the positrons themselves are detected, having undergone elastic collision, and coherently scattered back. Positron diffraction has features different from those of the diffraction of electrons (which are quantum mechanically indistinguishable from material electrons). It has been pointed out that these features may lead to the positron diffraction method being superior to the electron counterpart.[1,2,4] Perhaps the only drawback with using positrons is that, since it is an antiparticle, it is technically more difficult to obtain a beam of high intensity.

First proposed by Ichimiya[1] in 1992, RHEPD uses positrons of approximately 10 keV in energy and directs them at a crystal surface with a glancing angle smaller than typically 6°. The usefulness of this technique was proved by Kawasuso and Okada[2] in 1998 at JAEA, Takasaki, with an apparatus using a ^{22}Na positron source providing a beam of 10^3–10^4 slow positrons/s.

This apparatus, which was the only one of its kind in the world, and subsequent modifications of it, yielded fruitful results for more than a decade in determining the structures of metal-deposited surfaces of Si and Ge crystals,[5] some of which were impossible or very difficult to characterize by other techniques. Some notable examples are as follows. It was shown from the excellent fit of the data of the RHEPD rocking curves[6] that the arrangement of In atoms on a Si(111)-(8 × 2)-In surface at low temperatures was that of the hexagon model.[7] The details of the $(\sqrt{21} \times \sqrt{21})$ structure of noble metals (Ag, Au) deposited on Si(111)-$(\sqrt{3} \times \sqrt{3})$-Ag were determined using RHEPD rocking curves and the intensity profile along the 1/7 Laue zone.[8] The structure found was different from any of the models previously proposed.[9–12]

Recently, the RHEPD station has been moved to the Slow Positron Facility at KEK where an intense slow positron beam is produced using a dedicated linac (55 MeV, 600 W) and a production (i.e., converter/moderator) unit consisting of a Ta target and a W foil moderator.[13] The first experiment performed, prior to the brightness enhancement described below, was a study of a Ge(001)-(4 × 2)-Pt surface.[14] A number of different models had been proposed[15–17] for the one-dimensional structure of this surface and, using the RHEPD rocking curves obtained, we were able to determine which of these models is correct.[17]

The high intensity of the positron beam allowed the installation of a transmission-type brightness enhancement[18] unit upstream of the RHEPD chamber. Positrons, transported at an energy of 15 keV, were focused onto a 100-nm-thick W foil remoderator at an electrostatic potential of 10 kV. The positrons thus struck the foil at 5 keV, thermalizing inside and were subsequently reemitted from the other side at 10 keV with a brightness enhanced by about 1×10^3 times over the initial magnetically guided beam. This refined beam has a diameter of ~0.5 mm (FWHM), an energy spread of ~40 meV, an angular divergence of ~12 mrad, and a normalized emittance of ~0.01 cm rad eV$^{1/2}$.[19] The final positron intensity was 5×10^5 slow positrons/s. It yielded a clear positron diffraction pattern from a crystal surface. The sample is now oriented in real time while observing the phosphor screen behind MCP. An RHEPD pattern can be taken within 1 h and a set of those necessary for making a specular-spot rocking curve within 3 h. The brightness-enhanced beam has recently been used to confirm that

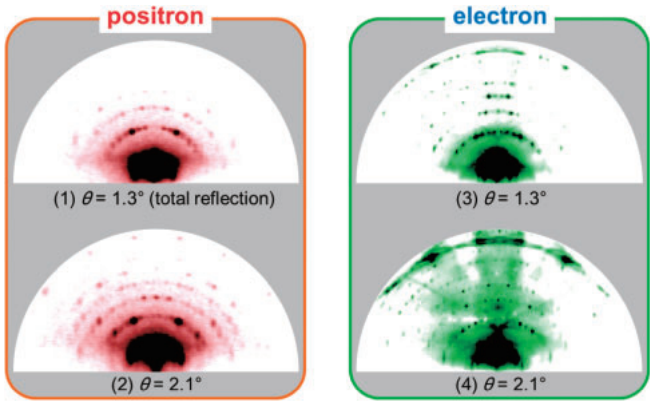

Fig. 1. Comparison between RHEPD (positron) and RHEED (electron) patterns of Si(111)-(7 × 7) surface. A darker contrast shows a higher intensity. The integer-order spots due to bulk diffraction are visible in the periphery of the RHEED patterns but not in the RHEPD pattern for $\theta = 1.3°$ (TRHEPD pattern). Kikuchi lines are much less prominent in the RHEPD patterns.

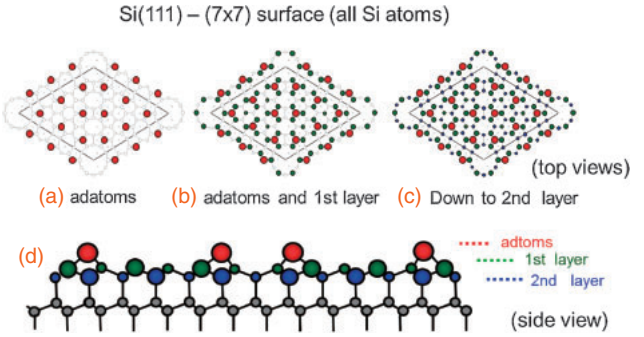

Fig. 2. Schematic diagram of Si(111)-(7 × 7) structure. The circles are all silicon atoms.

silicene constructed on a Ag(111) surface has a buckling structure[20] unlike graphene.

The advantage of RHEPD over RHEED is that it is capable of undergoing total reflection[1] owing to the positive crystal potential and is therefore particularly sensitive to the topmost atomic layer of the surface. The purpose of the present study is to show that the RHEPD patterns from a Si(111)-(7 × 7) surface for the total reflection condition do not contain contributions from atoms in the bulk. This surface was chosen to be a suitable testing ground since its structural characteristics are well known.[21,22] The critical glancing angle for the total reflection of 10 keV positrons from this surface is 2.0°. Note that the total reflection range covers a considerable part of a typical RHEPD measurement range (6°).

A Si(111) sample was cut from a mirror-polished n-type wafer with a resistance of 1–10 Ω cm. It was flushed at 1200 °C in an ultrahigh-vacuum chamber to produce a (7 × 7) reconstructed structure. The azimuth was chosen to be in the $[11\bar{2}]$ direction.

Figure 1 shows the RHEPD patterns observed for glancing angles θ of (1) 1.3° (within the total reflection condition, i.e., TRHEPD) and (2) 2.1° (slightly off the total reflection condition). The results of RHEED at the same energy and $\theta = 1.3°$ (3) and 2.1° (4) are also shown. The immediately apparent differences are as follows: (i) the intensity distributions of the spots are different; (ii) the integer-order spots due to bulk diffraction seen in the periphery of the RHEED patterns (3) and (4) are barely visible in the RHEPD pattern for $\theta = 1.3°$ (1); (iii) Kikuchi lines are noticeable only in the RHEED patterns (3) and (4). Observation (ii) indicates that, while RHEED contains information from the bulk crystal structure even at $\theta = 1.3°$, RHEPD for the same glancing angle gives information only from the surface. Observation (iii) is interpreted as follows. Because of the difference in the sign of the potential energy between the electron and the positron in the crystal, the index of refraction is larger than unity for the former and less than unity for the latter. When injected at the same glancing angle, the electron penetrates deeper and hence has more chance to undergo inelastic scattering relevant to the formation of the Kikuchi patterns than the positron.

To unambiguously show that the RHEPD patterns under total reflection conditions give only information about the atoms on the surface and not those in the bulk, we calculated the RHEPD patterns for the two glancing angles across the total reflection condition, together with the RHEED patterns for the same angles. Figure 2 is a schematic drawing of this surface in which the circles are all Si atoms. Shown are (a) the arrangement of adatoms (colored red), (b) the adatoms and first surface layer (colored green), and (c) down to the second surface layer (colored blue). Figure 2(d) shows a cross-sectional view of this surface structure.

Results of the calculations are shown in Fig. 3. The code developed by Ichimiya for the analysis of RHEED patterns on the basis of the dynamical electron diffraction theory[3,23] was adopted for RHEPD by changing the electric charge of the incident particle from negative to positive. Detailed positions of the atoms were taken from the ab initio calculation of this surface, i.e., the rumpling model, by Brommer et al.[22]

Figure 3(1) shows the calculated RHEPD pattern for $\theta = 1.3°$ (first data set). It can be clearly seen that the agreement of Fig. 3(1-d), calculated for the whole crystal, with the experimental data for $\theta = 1.3°$ in Fig. 1(1) is good. Figure 3(1-a) shows the RHEPD pattern for a two-dimensional single sheet of the Si(111)-(7 × 7) adatom configuration [Fig. 2(a)] calculated using the same code. Such a sheet cannot support itself in reality but it is possible to assume its existence for purposes of calculation. Interestingly, this calculated pattern [Fig. 3(1-a)] already displays most of the features shown in Figs. 3(1-d) and 1(1). This strongly indicates that the main features of both the experimentally observed pattern and the theoretical pattern calculated for the bulk sample are essentially determined by the contribution from the adatoms on the surface. If we look more closely at Figs. 3(1-a), 3(1-b), and 3(1-d), inclusion of the contributions from the atoms in the first surface layer gives a better agreement. This is reasonably understood if we note that the distribution of the Si adatoms in the (7 × 7) superstructure is rather sparse so that most of the atoms in the first surface layer (colored green) are also exposed, as can be seen in Figs. 2(b) and 2(d). Figure 3(1-c) is indistinguishable from Figs. 3(1-b) and 3(1-d), indicating that the atoms in the second surface layer have almost no contribution. The conclusion is that the RHEPD pattern in the total reflection condition for the Si(111)-(7 × 7) surface observed from a bulk sample includes only the contributions from the atoms exposed on the surface.

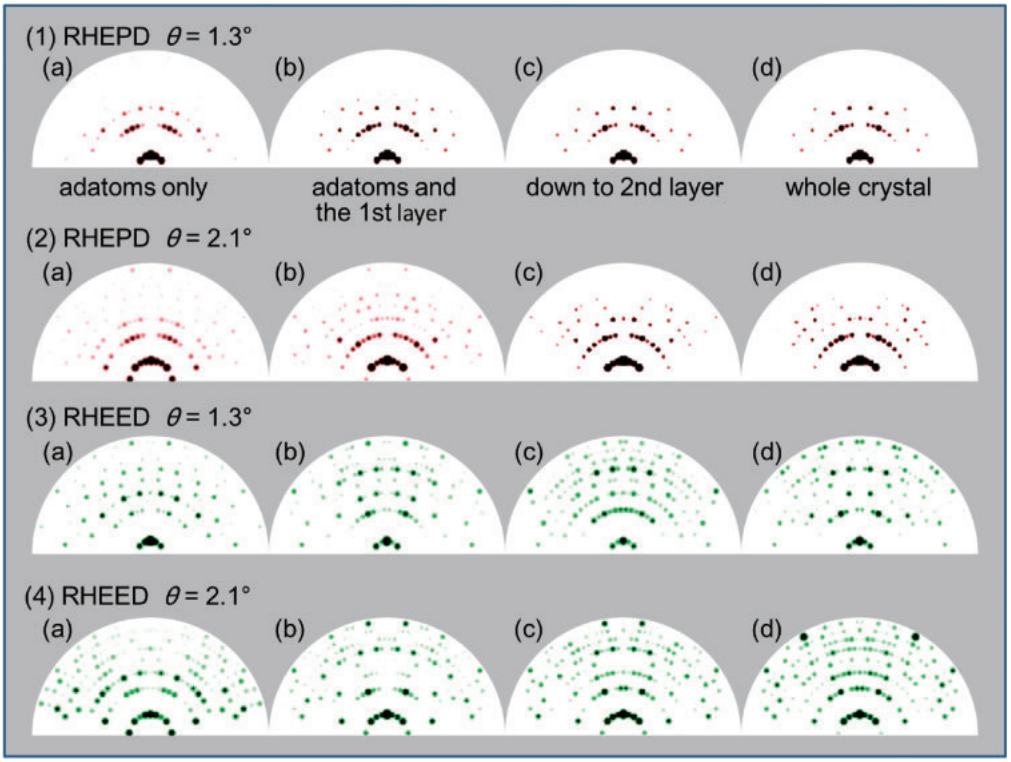

Fig. 3. RHEPD patterns for (1) glancing angle $\theta = 1.3°$ (within the total reflection condition), (2) $\theta = 2.1°$ (slightly off the total reflection condition), RHEED patterns for (3) $\theta = 1.3°$ and (4) $\theta = 2.1°$, calculated on the basis of the dynamical diffraction theory. A darker contrast shows a higher intensity. For each case, the results are shown for the assumed two-dimensional crystal sheet of the Si adatoms (a), as in Fig. 2(a); the set of sheets of adatoms and first surface layers (b), as in Fig. 2(b); the set of sheets of layers down to the second layer (c), as in Fig. 2(c); and for the whole crystal (d).

Figure 3(2) (second data set) shows similar results for $\theta = 2.1°$. In this data set also, Fig. 3(2-d) is the RHEPD pattern calculated for the bulk sample; Figs. 3(2-a)–3(2-c) are those for a single sheet of adatoms, and sheets down to the first and second layers, respectively. The effects of the inclusion of the second layer are clearly seen in Fig. 3(2-c), which is essentially the same as Fig. 3(2-d) and similar to Fig. 1(2). This indicates that the RHEPD pattern at this glancing angle includes contributions from the second layer, but almost no other contribution.

Results of the calculations for RHEED at $\theta = 1.3°$ are shown in Fig. 3(3) (third data set). The intensity distributions of all the patterns in this set are different from each other. This indicates that the pattern from the bulk sample by no means includes only the exposed atoms on the surface—a feature that is to be expected from the absence of the total reflection condition for electrons due to the positive crystal potential (negative potential energy for the electron). It is interesting that the RHEPD and RHEED patterns for $\theta = 1.3°$ are different for even the single sheet of adatoms. This indicates the existence of multiple scattering within the layer; since the phase shift in the individual scattering of the positron is different from that of the electron from a single Si atom, the multiple scattering yields the difference in the intensity of the spots.

Figure 3(4) (fourth data set) shows a similar analysis for the case of $\theta = 2.1°$. It reveals that contributions from many more layers are included at this glancing angle.

To quantify the above arguments, we introduce the residual factor R^* as a measure of the goodness of the agreement between the patterns calculated for a single sheet or a number of sheets of surface atomic layers and that calculated for the whole crystal:

$$R^* = \sum |f_{\text{sheet(s)}} - f_{\text{whole}}|/(f_{\text{sheet(s)}} + f_{\text{whole}}),$$

where f is the calculated intensity of the diffraction peak, after the normalization as $\sum f_{\text{sheet(s)}} = \sum f_{\text{whole}}$ for convenience of comparison, with the summations extended over all the peaks. A smaller R^* value indicates a closer agreement between the two calculated patterns. Note that the inclusion of a sufficient number of sheets that contribute to the diffraction pattern in the actual crystal will give $R^* = 0$. The results are shown in Fig. 4. It clearly shows that the RHEPD pattern for $\theta = 1.3°$ is almost entirely determined by the contributions from the adatoms and the atoms in the first surface layer, and that for $\theta = 2.1°$, by the atoms down to the second surface layer. In contrast, inclusion of the atomic layers down to the second surface layer in the case of RHEED is not enough to reproduce the pattern for the whole crystal. In more detail, inclusion of layers down to the second surface layer, (c), for $\theta = 1.3°$, does not appear to lower the R^* value from that for (b). This may seem strange because the pattern in Fig. 3(4-c) appears to resemble that in Fig. 3(3-d) more closely than that in Fig. 3(3-b). However, if we inspect them carefully, it is not the case, i.e., it so happens that some of the spots in the pattern in Fig. 3(3-b), which have a similar intensity to those in Fig. 3(3-d), reduce their intensities in Fig. 3(3-c), and in turn, some other spots gain a similar intensity to those in Fig. 3(3-d). This accidentally gives similar R^* values. Since diffraction patterns result from interference, a step-by-step inclusion of the surface layers does not necessarily improve the resemblance to the full inclusion monotonically. In fact,

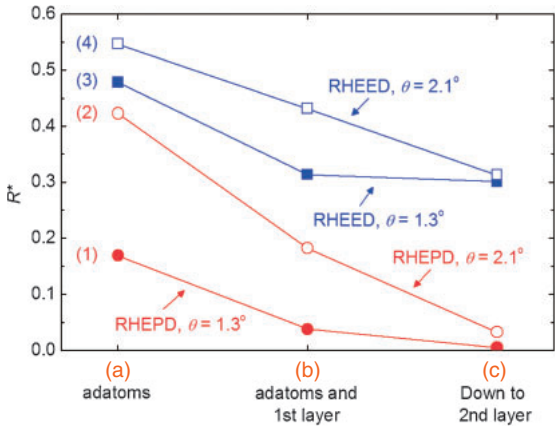

Fig. 4. Values of residual factor R^*, defined in the text, for RHEPD or RHEED patterns at glancing angles shown. This factor indicates the goodness of agreement between the patterns calculated for an assumed two-dimensional structure and the whole crystal; the smaller the value, the better the agreement. The assumed two-dimensional structures are as shown in (a) Fig. 2(a), (b) Fig. 2(b), and (c) Fig. 2(c). It is clearly seen that, in the case of (1), inclusion of the adatoms and the first surface layer reproduces very well the pattern calculated for the bulk crystal.

we have checked that if we further include the contribution from the third layer, R^* decreases to about 0.17.

In this study, we have demonstrated that RHEPD with a brightness-enhanced high-intensity positron beam has the promise to be an ideal tool for the determination of surface atomic configurations, where other more well-established methods are limited by physical and technical characteristics. This is the only technique that yields diffraction patterns separating out the contributions from the atoms exposed on the surface alone by simple measurements on a bulk sample. Furthermore, it should be possible to determine accurately the crystal structure of the surface region from the topmost layer downward by analyzing the RHEPD patterns across the total reflection range. Diminution of the Kikuchi patterns reduces the diffuse background and makes the accurate determination of the intensity of the spots easy. We propose to call this method using RHEPD data taken under the total reflection condition, total reflection high-energy positron diffraction (TRHEPD). We expect the application of this technique to play as significant a role in surface science as X-ray diffraction has played in solid-state physics and molecular biology.

Part of the present results were presented at SLOPOS-13 (13th International Workshop on Slow Positron Beam Technology and Applications).[24)]

Acknowledgments We thank the staff of the Photon Factory and the Accelerator Laboratory of KEK for their support in the operation of the Slow Positron Facility. This work has been supported by a Grant-in-Aid for Scientific Research (S) No. 24221007 and for Young Scientists (B) 25800182 from the Japan Society for the Promotion of Science.

1) A. Ichimiya, Solid State Phenom. **28–29**, 143 (1992).
2) A. Kawasuso and S. Okada, Phys. Rev. Lett. **81**, 2695 (1998).
3) A. Ichimiya and P. I. Cohen, *Reflection High-Energy Electron Diffraction* (Oxford University Press, Oxford, U.K., 2004).
4) S. T. Tong, Surf. Sci. **457**, L432 (2000).
5) Y. Fukaya, M. Maekawa, I. Mochizuki, K. Wada, T. Hyodo, and A. Kawasuso, J. Phys.: Conf. Ser. **443**, 012068 (2013).
6) Y. Fukaya, M. Hashimoto, A. Kawasuso, and A. Ichimiya, Surf. Sci. **602**, 2448 (2008).
7) C. González, F. Flores, and J. Ortega, Phys. Rev. Lett. **96**, 136101 (2006).
8) Y. Fukaya, A. Kawasuso, and A. Ichimiya, Surf. Sci. **600**, 3141 (2006).
9) A. Ichimiya, H. Nomura, Y. Horio, T. Sato, T. Sueyoshi, and M. Iwatsuki, Surf. Rev. Lett. **1**, 1 (1994).
10) J. Nogami, K. J. Wan, and X. F. Lin, Surf. Sci. **306**, 81 (1994).
11) X. Tong, Y. Sugiura, T. Nagao, T. Takami, S. Takeda, S. Ino, and S. Hasegawa, Surf. Sci. **408**, 146 (1998).
12) H. Tajiri, K. Sumitani, W. Yashiro, S. Nakatani, T. Takahashi, K. Akimoto, H. Sugiyama, X. Zhang, and H. Kawata, Surf. Sci. **493**, 214 (2001).
13) K. Wada, T. Hyodo, A. Yagishita, M. Ikeda, S. Ohsawa, T. Shidara, K. Michishio, T. Tachibana, Y. Nagashima, Y. Fukaya, M. Maekawa, and A. Kawasuso, Eur. Phys. J. D **66**, 37 (2012).
14) I. Mochizuki, Y. Fukaya, A. Kawasuso, K. Yaji, A. Harasawa, I. Matsuda, K. Wada, and T. Hyodo, Phys. Rev. B **85**, 245438 (2012).
15) O. Gürlu, O. A. O. Adam, H. J. W. Zandvliet, and B. Poelsema, Appl. Phys. Lett. **83**, 4610 (2003).
16) A. A. Stekolnikov, F. Bechstedt, M. Wisniewski, J. Schafer, and R. Claessen, Phys. Rev. Lett. **100**, 196101 (2008).
17) D. E. P. Vanpoucke and G. Brocks, Phys. Rev. B **77**, 241308(R) (2008).
18) D. M. Chen, K. G. Lynn, R. Pareja, and B. Nielsen, Phys. Rev. B **31**, 4123 (1985).
19) M. Maekawa, K. Wada, Y. Fukaya, A. Kawasuso, I. Mochizuki, T. Shidara, and T. Hyodo, to be published in Eur. Phys. J. D (2014).
20) Y. Fukaya, I. Mochizuki, M. Maekawa, K. Wada, T. Hyodo, I. Matsuda, and A. Kawasuso, Phys. Rev. B **88**, 205413 (2013).
21) K. Takayanagi, Y. Tanishiro, M. Takahashi, and S. Takahashi, Surf. Sci. **164**, 367 (1985).
22) K. D. Brommer, M. Needels, B. E. Larson, and J. D. Joannopoulos, Phys. Rev. Lett. **68**, 1355 (1992).
23) A. Ichimiya, Jpn. J. Appl. Phys. **22**, 176 (1983).
24) T. Hyodo, Y. Fukaya, M. Maekawa, I. Mochizuki, K. Wada, T. Shidara, A. Ichimiya, and A. Kawasuso, to be published in J. Phys.: Conf. Ser. (2014).